

# A modified elasto-viscoplastic thixotropic model for two commercial gelled waxy crude oils

Charlie Van Der Geest<sup>1</sup> · Vanessa C. Bizotto Guersoni<sup>2</sup> · Daniel Merino-Garcia<sup>3</sup> · Antonio C. Bannwart<sup>1</sup>

Received: 4 September 2014 / Revised: 23 February 2015 / Accepted: 11 March 2015 / Published online: 18 April 2015  
© Springer-Verlag Berlin Heidelberg 2015

**Abstract** A severe problem to flow assurance occurs when subsea flowlines become blocked with gelled waxy crudes. To design proper surface pump facilities, it is essential to know the minimum pressure required to restart the flow. Simulating and predicting this minimum pressure require the understanding of several physical phenomena, including compressibility, shrinkage, and rheological behavior. This study aims to characterize and simulate the rheological behavior of two commercial waxy crude oils. Based on its survey of the literature, we select the de Souza Mendes and Thompson (2013) model to fit the oil's behavior and then conduct, using a rheometer, a considerable number of experiments with the selected oils. To verify the solution of our algorithm, we compared our theoretical solutions with some results of the literature. When comparing the simulation with experiments, the model was unable to predict the data perfectly; hence, we propose a modified version without changing the physical meaning of the equations, to improve its predictions. Once any of the empirical parameters were able to influence the elastic behavior in such a way that the shear stress

decreased with time, the structural elastic modulus function was modified, which means that the relation of the structure parameter and the storage modulus was modified. One of the interesting results of the analysis is when relating the storage modulus and a new parameter added in the modification, a value was found to be, regardless of the aging time or the oil used, constant.

**Keywords** Waxy crude oil · Rheological model · Yield stress

## Nomenclature: Roman symbols

$a, b, m$	Empirical parameters
C	Atom of carbon
H	Atom of hydrogen
$t_{eq}$	Equilibrium time (s)
$n$	Herschel-Bulkley exponential term
$k$	Herschel-Bulkley apparent viscosity (Pa.s)
$G_0$	Storage modulus of the completely structured material (Pa)
$G_s$	Structural elastic modulus (Pa)
$G'$	Storage modulus (Pa)
$G''$	Loss modulus (Pa)

## Greek symbols

$\lambda$	Structure parameter
$\lambda_0$	Initial value of the structure parameter
$\lambda_{eq}$	Structure parameter at equilibrium
$\gamma$	Strain (m)
$\gamma_e$	Elastic strain (m)
$\gamma_v$	Viscous strain (m)
$\tau$	Shear stress (Pa)
$\tau_y$	Static limit of the shear stress (Pa)
$\tau_{yd}$	Dynamic shear stress (Pa)
$\dot{\gamma}$	Shear rate ( $s^{-1}$ )
$\dot{\gamma}_1$	Transition shear rate from static to viscous ( $s^{-1}$ )

✉ Charlie Van Der Geest  
charlievander@gmail.com

Vanessa C. Bizotto Guersoni  
vanessa@cepetro.unicamp.br

Daniel Merino-Garcia  
dmerinog@repsolsinopec.com

Antonio C. Bannwart  
bannwart@fem.unicamp.br

<sup>1</sup> School of Mechanical Engineering, University of Campinas, Campinas 13083-860, Brazil

<sup>2</sup> Center for Petroleum Studies, University of Campinas, UNICAMP, Campinas 13083-970, Brazil

<sup>3</sup> Repsol Sinopec Brazil, Rio de Janeiro 22250-040, Brazil

$\eta$	Apparent viscosity (Pa.s)
$\eta_{\infty}$	Purely viscous (Pa.s)
$\eta_s$	Structural viscosity (Pa.s)
$\eta_v$	Addition of $\eta_{\infty}$ and $\eta_s$ (Pa.s)
$\eta_0$	Initial viscosity (Pa.s)
$\eta_{eq}$	Viscosity at equilibrium (Pa.s)
$\theta_1$	Relaxation time (s)
$\theta_2$	Retardation time (s)

## Introduction

Crude oils are a complex mixture of hydrocarbons in which the majorities are saturated alkanes. In some cases, the concentration of high molecular linear alkanes is very high, leading to the appearance of solids when fluids are cooled below a threshold temperature, termed wax appearance temperature (WAT); in these cases, the fluids are typically called waxy oils. The wax fraction of the oil comprises the molecules that are expected to solidify upon temperature decrease and typically contain molecules with alkyl chain length greater than 18 units. The percentage of such hydrocarbons in oils worldwide usually ranges from 1 to 50 % (Ajienka and Ikoku 1991).

Oil production in the next decades will have a greater contribution from subsea environments, where ambient temperature is as low as 3–4 °C. Consequently, problems associated to solid appearance at low temperatures (such as waxes and hydrates) are becoming more significant. Flow assurance problems associated to waxes range from increased pressure drop, mainly because of diameter reduction, and line blockages. As

remediation costs are quite high, there is a trend in the last decades to develop predictive methods for wax deposition and gelation of the crude oil (Srivastava et al. 1993; Chang et al. 1998, 1999; da Silva and Coutinho 2004; Lee 2008; Luthi 2013).

While wax deposition during flow has advanced to the degree of developing predictive models, the restart of the flow in a pipe full of gelled waxy crude still lacks a commercial tool that is capable of describing the phenomena in its full complexity. When prolonged shutdowns (planned or unplanned) occur, the resultant loss of heat leads to the gelation of the oil when temperature drops below its pour point. The literature has several examples of attempts of generating models to predict the restart of the flow in these conditions (Davidson et al. 2004; Vinay et al. 2009; Phillips et al. 2011a, b).

When designing the pipelines and the pump facilities, engineers usually do a simplified force balance. The assumption is that when the pressure is enough to overcome the yield stress, the restart occurs. The problem is that there is evidence that this calculation is overestimated; therefore, a better rheological modeling of these oils is necessary once they present an “elasto-viscoplastic thixotropic” behavior, which is a complex mixture of plasticity, elasticity, and thixotropy.

For a number of years, researchers have discussed the concept of yield stress, with Barnes and Walters (1985) going so far as to call its definition a myth. For engineering concerns, however, the notion of yield stress is quite useful, capable, as de Souza Mendes and Thompson (2013) pointed out, of predicting the behavior of real fluids. On the other hand,

**Fig. 1** Steady-state curve for oil 1 after 1 h of aging

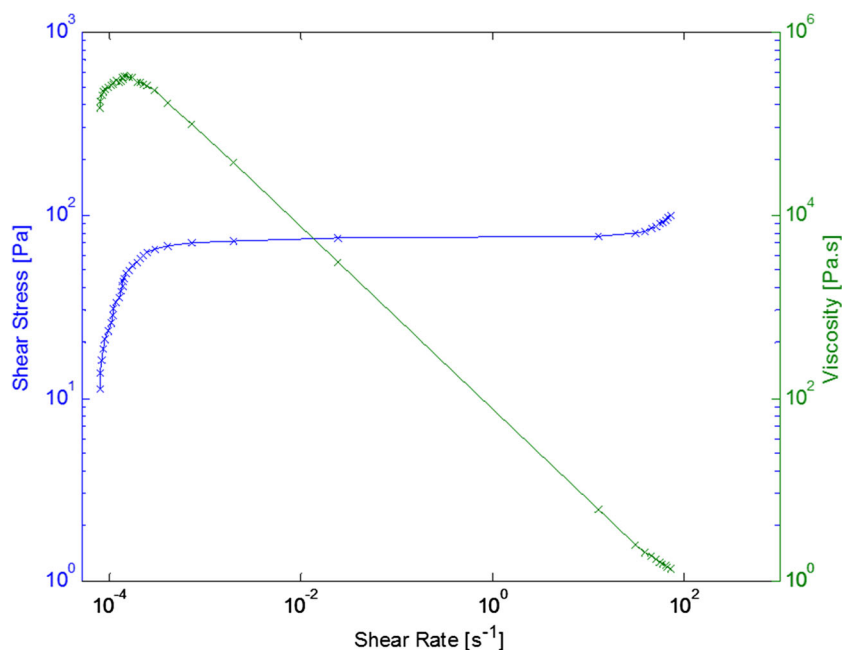
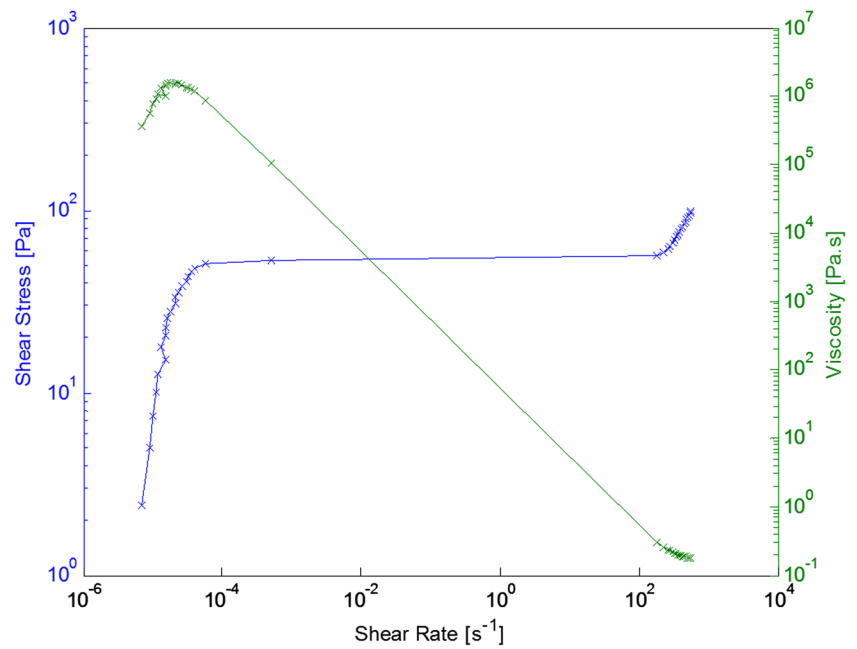


**Fig. 2** Steady-state curve for oil 2 after 1 h of aging



thixotropic behavior has received varied definitions along history. For instance, *The Oxford Encyclopedic Dictionary of Physics* (Thewlis 1962) says:

Certain materials behave as solids under very small applied stresses but under greater stresses become liquids. When the stresses are removed the material settles back into its original consistency. This property is particularly associated with certain colloids which form gels when

left to stand but which become sols when stirred or shaken, due to a redistribution of the solid phase.

In this manuscript, we present a study on the rheological behavior and the attempt on modeling two commercial gelled waxy crudes. First, there is a full rheological characterization of the oils. Second, we show an attempt to predict the data with an elasto-viscoplastic thixotropic model proposed by de Souza Mendes and Thompson (2013), and finally, as the

**Fig. 3** Stress sweep curve for oil 1 at 1 Hz without aging time

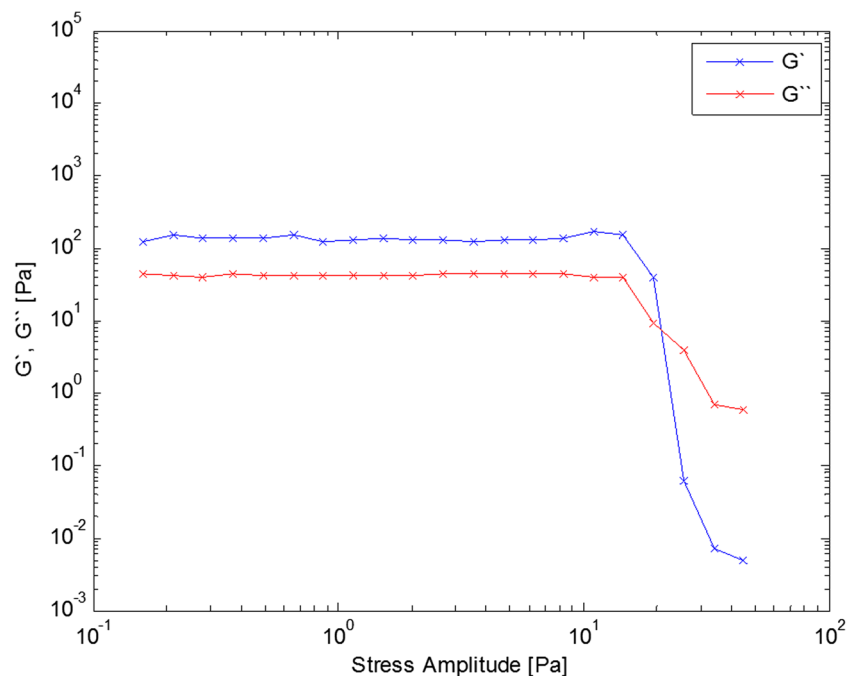
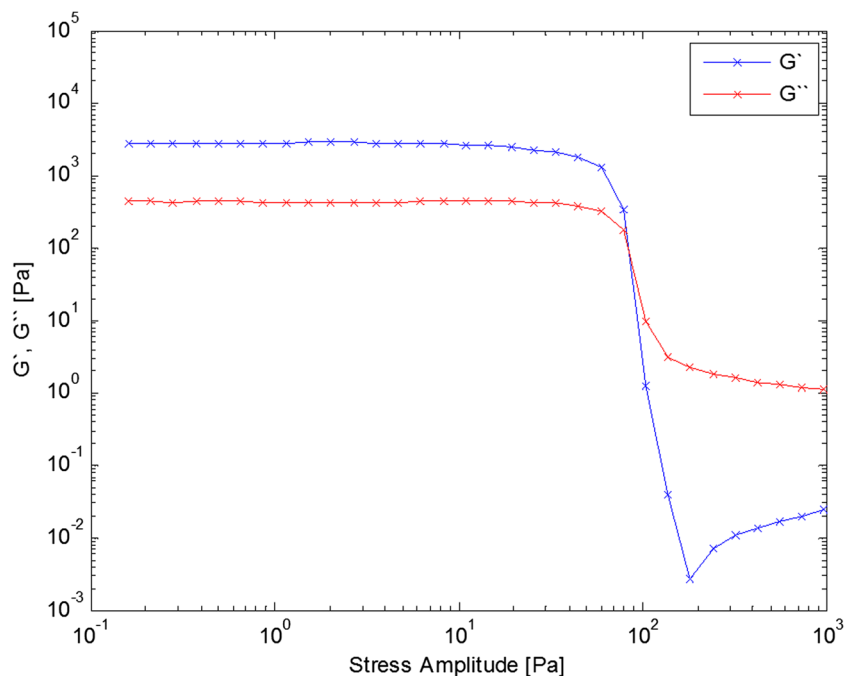


**Fig. 4** Stress sweep curve for oil 2 at 1 Hz without aging time



model could not predict the data, we modified one equation, which produced satisfactory results.

### Rheological characterization

Two waxy crude oil samples were used in this study (oil 1 and 2). They are oil samples that have been stabilized to eliminate, from the results, the impact of light ends. The difference between them is the weight percentages of high molecular

weight n-paraffins, approximately 5 and 10 %, for oil 1 and oil 2, respectively.

### Test procedure

All experiments were performed in a controlled-stress rheometer (MARS III from HAAKE GmbH), using a cone and plate geometry with a diameter of 60 mm and a cone angle of  $1^\circ$ . Luthi (2013) showed that this geometry could be used because the size of paraffin crystals are reasonably smaller ( $2 \mu\text{m}$ ) than

**Fig. 5** Constant shear rate flow for oil 1 and 1 h of aging time

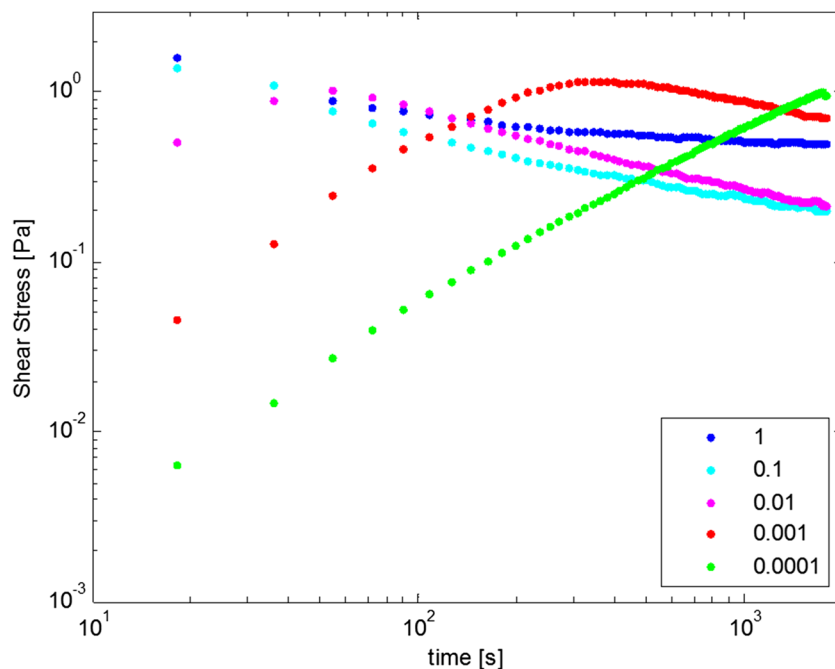
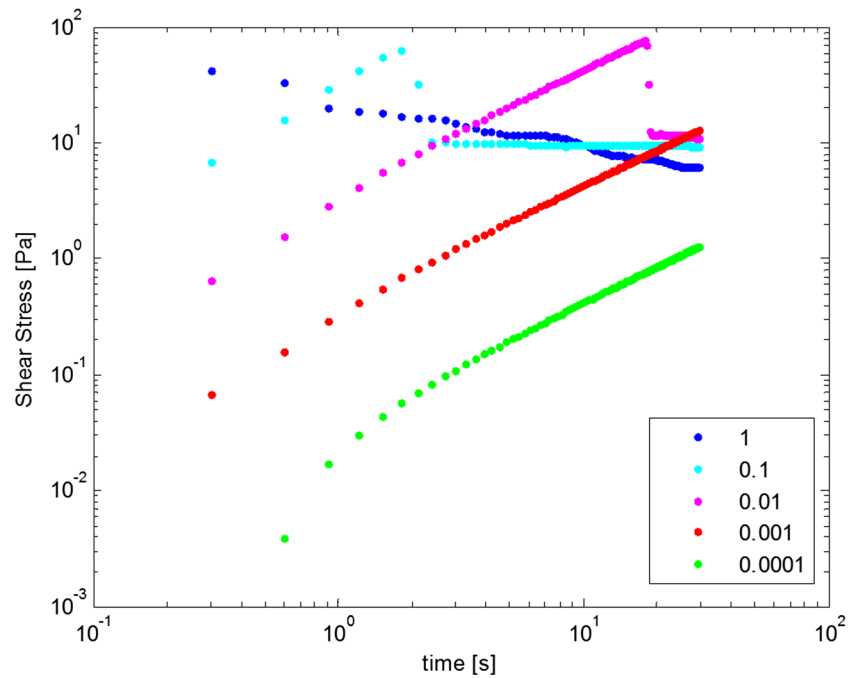


**Fig. 6** Constant shear rate flow for oil 2 and 1 h of aging time

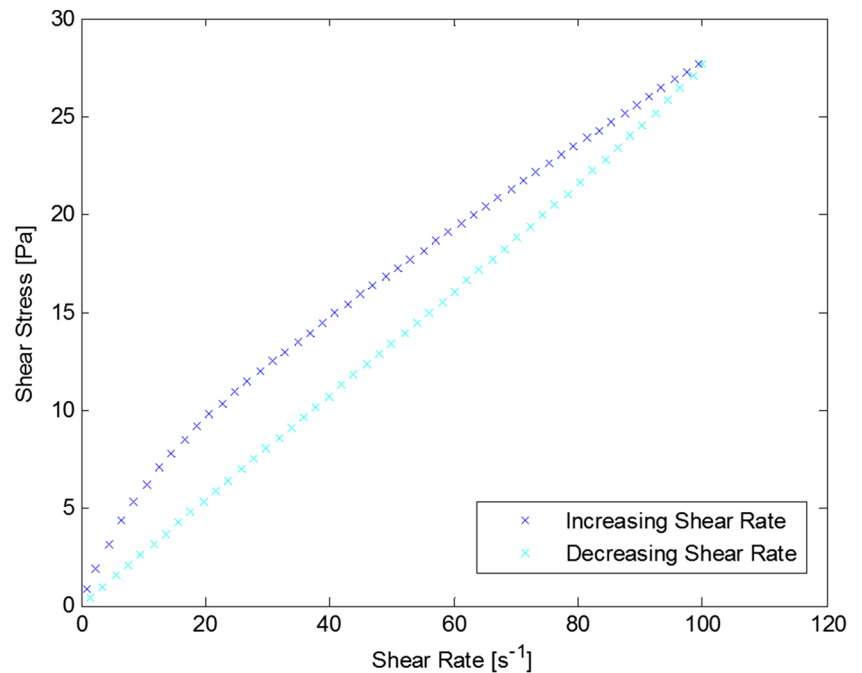


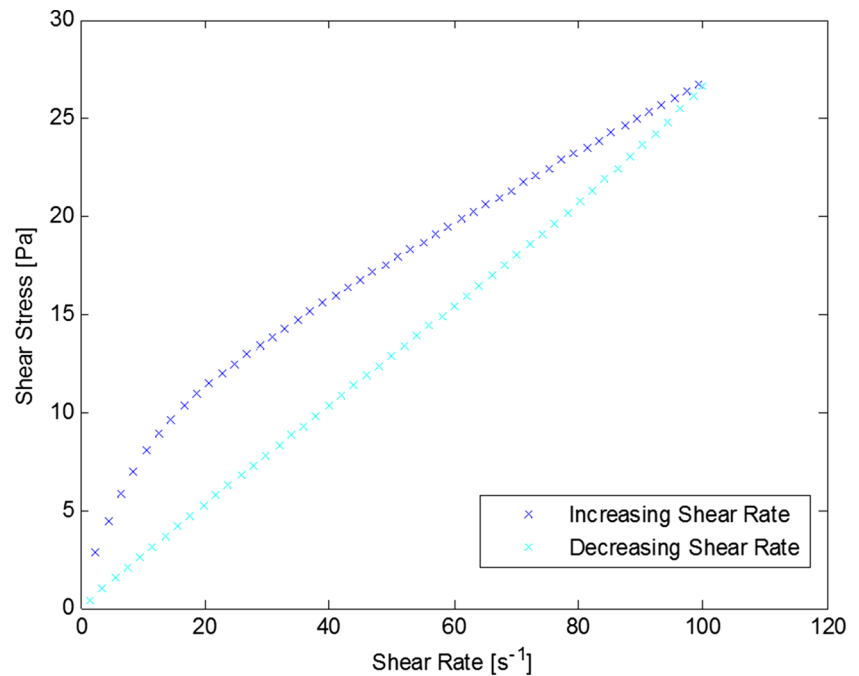
the gap (0.052 mm); thus, the results are independent from crystal size. Sample's temperature and cooling rate were controlled using the rheometer Peltier plate. The gap was adjusted with the thermogap option, which means that as the fluid shrinks, the rheometer would decrease the size of the gap to keep in touch with the fluid surfaces.

The initial procedure was adopted for all rheological analysis: We preheated the samples in a closed bottle to 70 °C and maintained at that temperature for 2 h. This

step ensured a stable chemical composition and achieved, therefore, reproducibility of the data. At 70 °C, the oil temperature is above of wax appearance temperature (WAT), determined by differential scanning calorimetry (DSC). Samples were then put in the rheometer, kept at 70 °C and at a shear rate of 10 s<sup>-1</sup> for 10 min to erase thermal history effects. Finally, the samples were cooled statically to 5 °C at a rate of 1 °C/min and left at rest for aging times of 1, 5, and 24 h.

**Fig. 7** Thixotropic loop for oil 1



**Fig. 8** Thixotropic loop for oil 2

### Flow curve

This result represents the steady-state shear stress and viscosity as a function of the shear rate. Figures 1 and 2 display the experimental data after 1 h of aging for oil 1 and oil 2, respectively. The data was obtained in triplicate, with accuracy.

In both experiments, it is possible to see what looks like an elastic behavior before the yield stress. Barnes and Walters (1985) argued that a material that appears to have a yield stress, if you have the technology or the time to apply the stress for long enough time, you will actually see a deformation of the material. After the apparent yield stress is reached, it is possible to verify the viscoplastic behavior of Herschel-Bulkley for both the oils.

### Oscillatory flow

The oscillatory test is a classic way to quantifying the behavior of viscoelastic materials, by verifying the elastic (linear region) response of the material.

After samples had reached 5 °C, oscillation stress sweep was performed at 1 Hz, applying stress values ranging from 0.01 to 1000 Pa. Figures 3 and 4 show the results of oil 1 and oil 2, respectively.

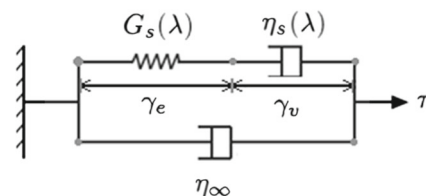
This test allows verifying the storage modulus, the loss modulus during the elastic region. The elastic shear stress and the static shear stress in the yielding region (Chang et al. 1998).

### Constant shear rate flow

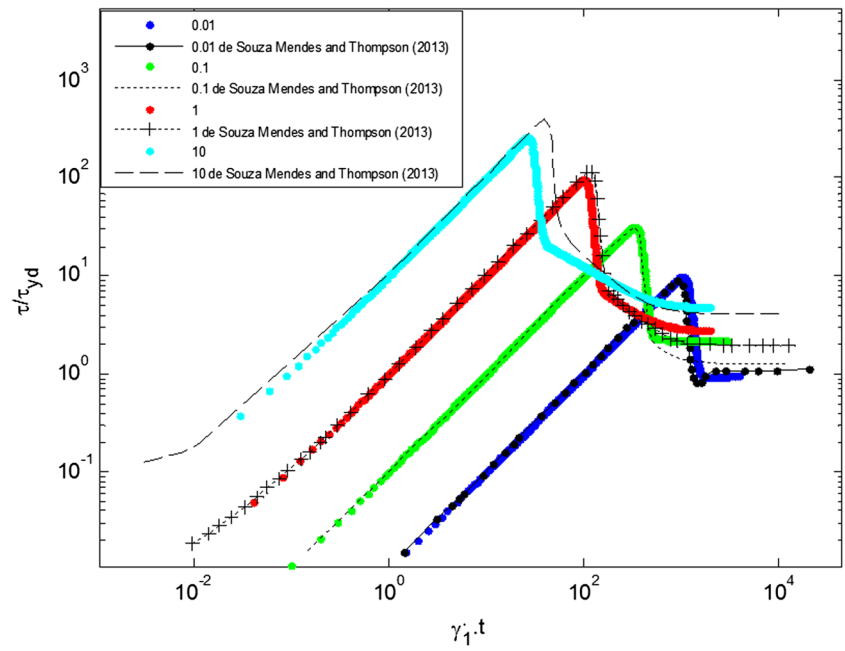
Applying a constant shear rate will result in an overshoot stress followed by decay towards the steady-state value. This decay can be abrupt or gradual, depending on the amount of wax and the kind of failure that is happening. For higher aging time, the stress overshoot is greater because the gel is more structured and rigid and a delay time is observed to break up the gel in comparison with aging the time 1 h.

Both crudes behave similarly. Figures 5 and 6 show the result for oil 1 and oil 2, respectively. The higher stress required by oil 2 can be explained by the fact that this crude has higher paraffin content than oil 1. A time-independent fluid would exhibit constant shear stress for every shear rate.

Before the overshoot, the fluid behaves elastically. The overshoot is usually caused by the thixotropic behavior, because the microstructure starts to break down and a fluid with massive viscosity starts to flow.

**Fig. 9** Physical analogy of de Souza Mendes and Thompson's (2013) model

**Fig. 10** Time evolution of stress for constant shear-rate flows; comparing results of de Souza Mendes and Thompson (2013) with the Euler’s method used in this manuscript



**Thixotropic loop**

One way to quantify the thixotropy is to verify the hysteresis of the material. A thixotropic loop is an experiment that measures the stress while the shear rate rises and decreases.

After the samples reached 5 °C in the rheometer, a shear rate of 1  $s^{-1}$  was applied for 60 s and then increased to 100  $s^{-1}$  and immediately decreased to 1  $s^{-1}$ .

The result of this experiment is similar to the flow curve; the difference is that the structure was destroyed by applying 1 min of shear rate before starting to measure. That is why there is no yield stress in the beginning of the experiment.

The existence of hysteresis for both oils is clear as indicated in Figs. 7 and 8, which represents a thixotropic behavior. One of the ways to quantify the thixotropy is to calculate the area inside the loop.

**Fig. 11** Steady-state shear stress curves and Herschel-Bulkley simulation for oil 1

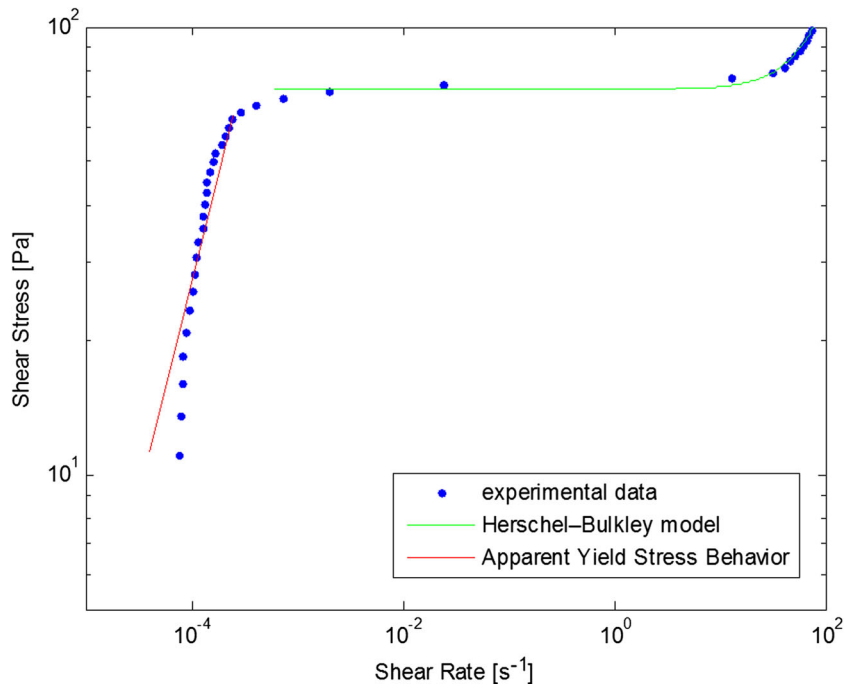
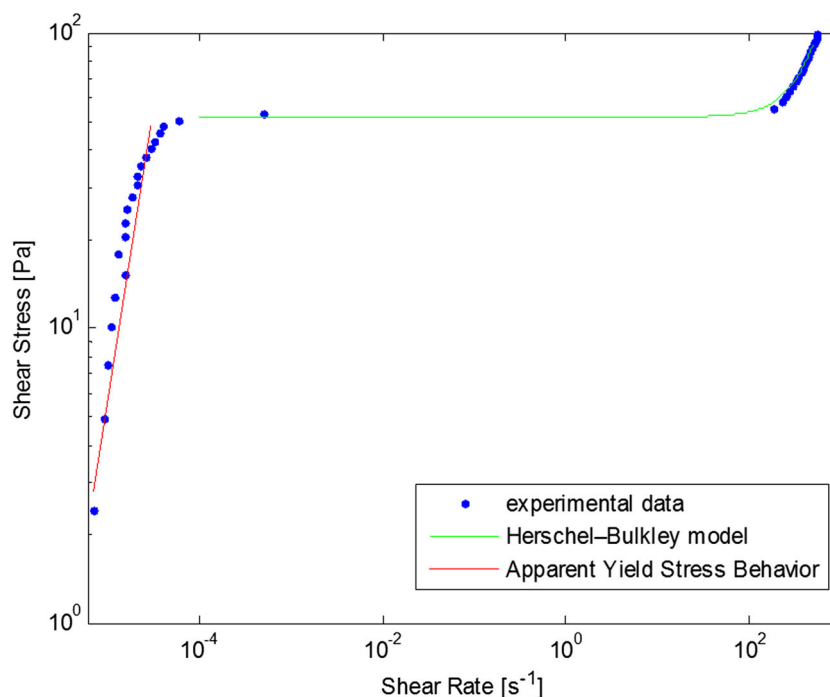


**Fig. 12** Steady-state shear stress curves and Herschel-Bulkley simulation for oil 2



## Rheological models

With the results presented in the last section, it is possible to verify that gelled crudes have complex rheological behavior. The flow curves show an apparent yield stress. Oscillatory test shows a change on the behavior from solid-like to liquid-like. The dynamic curves with constant shear rate show an overshoot of the stress. Finally, the thixotropic loop shows a change on the viscosity with time.

Many models in the literature try to predict complex behavior including thixotropy, elasticity, and plasticity (Slibar and Paslay 1963; Tiu and Boger 1974; Toorman 1997; Chang et al. 1999; Dullaert and Mewis 2005; Dullaert and Mewis 2006; Mewis and Wagner 2009; de Souza Mendes 2011; de Souza Mendes and Thompson 2013). There are a few reviews on those models (Mewis 1979; Barnes 1997, 1999; Mujumdar et al. 2002; de Souza Mendes and Thompson 2012). The Dullaert and Mewis (2005) and de Souza Mendes and Thompson

(2013) are among the most common ones. We used the model of de Souza Mendes and Thompson (2013) in this study because it has a plausible physical explanation based on a mechanical analog and possesses an equation for the structure parameter dependent on shear stress, while the structure parameter equation of Dullaert and Mewis (2005) is dependent only on the shear rate.

In fact, the structure should mainly depend on shear stress. This argument can be illustrated through the following example: If a small stress is applied to a structured oil, it will undergo a strain. If it stays within the elastic behavior, then once the stress stops, the oil should restructure. If, on the other hand, the applied stress stays long enough, the structure could reach a point where it starts to break down, and the yield stress itself decreases. Then, and only then, a fluid-like behavior is observed, giving rise to shear rate. That is why the model of Dullaert and Mewis cannot predict constant shear stress experiments.

**Table 1** Parameters obtained from steady-state test, oil 1

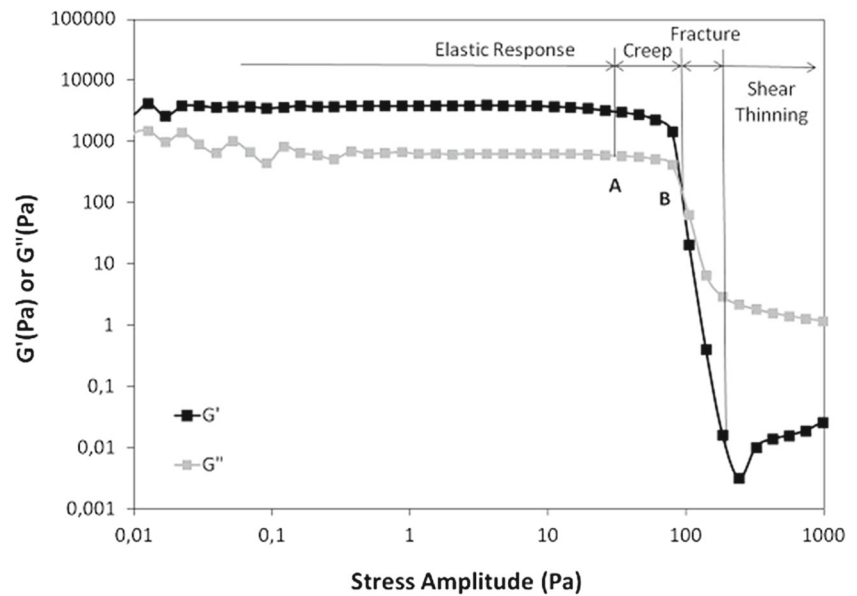
Parameters	Values	Units
$K$ (Herschel-Bulkley)	$2.1 \cdot 10^{-2}$	Pa. $s^n$
$n$ (Herschel-Bulkley)	1.7	–
$\eta_0$	$10^5$	Pa. s
$\tau_{yd}$	0.2	Pa
$\dot{\gamma}_{yd}$	$6.10^{-4}$	$s^{-1}$

**Table 2** Parameters obtained from steady state test, oil 2

Parameters	Values	Units
$K$ (Herschel-Bulkley)	$0.32 \cdot 10^{-3}$	Pa. $s^n$
$n$ (Herschel-Bulkley)	1.89	–
$\eta_0$	$10^6$	Pa. s
$\tau_{yd}$	10	Pa
$\dot{\gamma}_{yd}$	$10^{-4}$	$s^{-1}$



**Fig. 13** Stress sweep curve for oil 2 at 1 Hz without aging time



**The de Souza Mendes and Thompson (2013) model**

Given that a full discussion of the generalization of classical rheological models is available elsewhere (de Souza Mendes and Thompson 2012), we only briefly describe here the physical understanding of this complex rheological model. The model is based on an analogy between the viscoelastic behavior and a mechanical analog with springs and dampers, as illustrated in Fig. 9. The solid-like behavior can be compared to a spring and the liquid-like behavior to dampers. When viscosity is at its highest point (oil fully structured), the rheological behavior is dominated by the spring-like component. When viscosity is low (no structure), the rheological behavior is dominated by the damper-like component, creating resistance to flow.

Parameter  $\lambda$  represents the structure of the gel network that the fluid generates below the pour point. This dimensionless parameter is common to all models that are considered as “indirect micro-structural approaches” (Mujumdar et al. 2002).

Typically, when a gel is fully structured,  $\lambda$  is equal to 1 and, as the gel loses structure and behaves more liquid-like, this value approaches zero. The model proposed by de Souza Mendes and Thompson, however, uses a different approach. They considered the fully structured fluid ( $\lambda_0$ ) to depend on the initial and final viscosity. This is further described below.

With this structural dimensionless parameter, the model is able to account for the thixotropy, elasticity, plasticity, and viscous behavior of waxy oil. The next section lays out the main components of the model.

The constitutive equation comes from the description of the stress and strain in the system, as shown in Eq. (1).

$$\frac{\theta_2}{\eta_\infty} \left( \frac{\tau}{\theta_1} + \dot{\tau} \right) = (\dot{\gamma} + \theta_2 \ddot{\gamma}) \tag{1}$$

Equation (1) relates the stress  $\tau$ , the derivative of stress versus time  $\dot{\tau}$ , with the shear rate  $\dot{\gamma}$  and the derivative of shear rate versus time  $\ddot{\gamma}$ . There are two new terms relaxation time ( $\theta_1$ ) and retardation time ( $\theta_2$ ). Equations (2) and (3) are their respective mathematical definitions (de Souza Mendes 2011).

$$\theta_1 = \left( 1 - \frac{\eta_\infty}{\eta_v(\lambda)} \right) \frac{\eta_v(\lambda)}{G_s(\lambda)} \tag{2}$$

$$\theta_2 = \left( 1 - \frac{\eta_\infty}{\eta_v(\lambda)} \right) \frac{\eta_\infty}{G_s(\lambda)} \tag{3}$$

1) The structural elastic modulus function

Parameter  $G_s(\lambda)$  is defined as the shear modulus. It is related to the storage modulus ( $G_0$ ), and it represents the

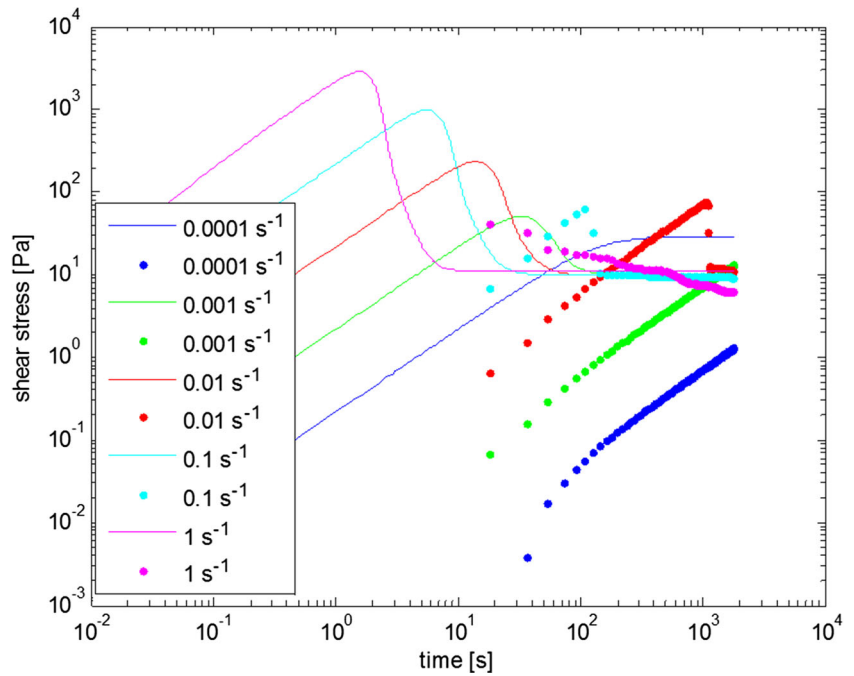
**Table 3** Parameters obtained from the oscillatory tests for oil 1

Parameters	Values	Units
$\eta_\infty$	0.1	Pa. s
$\tau_y$	8	Pa
$G_0$	100	Pa

**Table 4** Parameters obtained from the oscillatory tests for oil 2

Parameters	Values	Units
$\eta_\infty$	1.05	Pa. s
$\tau_y$	122	Pa
$G_0$	2200	Pa

**Fig. 14** Experimental and simulation of oil 2 using the empirical parameters by de Souza Mendes and Thompson (2013)



“variation of the elastic constant factor” of the spring.  $m$  is an empirical parameter.

$$G_s = G_0 e^{m \left( \frac{1}{\lambda} - \frac{1}{\lambda_0} \right)} \tag{4}$$

2) The structural viscosity function

The  $\eta_s$  is the structural viscosity, represented by a function of the viscous response of the microstructure. The last physical term in Fig. 9 is  $\eta_\infty$ , representing purely viscous behavior (i.e.,  $\lambda=0$ ). It is necessary to represent the fact that when  $G_s \rightarrow \infty$ , a purely viscous behavior has been attained. At such conditions, viscosity is calculated as  $\eta_v = \eta_s + \eta_\infty$ .

In Eq. (5), there is a correlation of structural viscosity function with the structure parameter  $\lambda$  and the purely viscous component  $\eta_\infty$ . A full discussion of the physical meaning can be found elsewhere (de Souza Mendes and Thompson 2013).

$$\eta_v(\lambda) = \eta_\infty e^\lambda \tag{5}$$

The next phenomenon to be described is the equilibrium state, also known as steady state. Such a state arises when buildup and breakdown rates are equal. The flow curve is the result of achieving this point for each shear rate. Equation (6) shows the equilibrium structure parameter.

$$\lambda_{eq} = \ln \left( \frac{\eta_{eq}}{\eta_\infty} \right) \tag{6}$$

The domain of the viscosity  $\eta_v(\lambda) \rightarrow [\eta_\infty, \eta_0]$  is directly proportional to the structure parameter  $\lambda \rightarrow [0, \lambda_0]$ . Hence, it

is possible to define the initial structure parameter that has been discussed earlier, shown in Eq. (7).

$$\lambda_0 = \ln \left( \frac{\eta_0}{\eta_\infty} \right) \tag{7}$$

Finally, Eq. (8) describes the variation of the viscosity in steady state. This equation is used later to match experimental data.

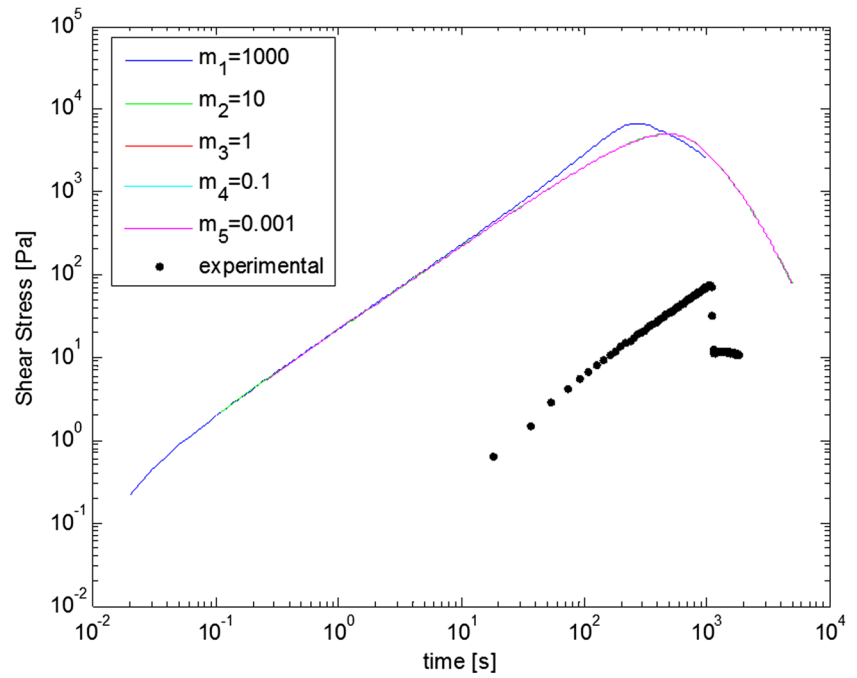
$$\eta_{eq}(\dot{\gamma}) = \left( 1 - e^{-\frac{m\dot{\gamma}}{\tau_y}} \right) \left( \frac{\tau_y - \tau_{yd}}{\dot{\gamma}} e^{-\frac{\dot{\gamma}}{\dot{\gamma}_{yd}}} + \frac{\tau_{yd}}{\dot{\gamma}} + K\dot{\gamma}^{n-1} \right) + \eta_\infty \tag{8}$$

There are a number of variables in this equation yet to be explained. They are related to the steady state. The  $\tau_y$  is the static limit of the stress. That is to say, it is the point at which the fluid will stop behaving like a solid and start behaving like a liquid. The second parameter is  $\tau_{yd}$ , the dynamic stress, which is the shear stress caused by the flow after the structure has been totally degraded. The point of transition from  $\tau_y$  to  $\tau_{yd}$  is  $\dot{\gamma}_{yd}$ , which is the shear rate that represents the change from the solid-like behavior to the liquid-like behavior,

**Table 5** Empirical parameters reported in de Souza Mendes and Thompson (2013)

Parameters	Values	Units
$m$	1	–
$a$	1	–
$b$	1	–
$t_{eq}$	100	s

**Fig. 15** Analysis of the influence of the empirical parameter  $m$  for the shear rate of  $0.01 \text{ s}^{-1}$



where the viscous behavior is dominant. That does not mean that the structure is completely destroyed, only that the viscous flow becomes predominant.

The last two parameters  $k$  and  $n$  are related to the classical viscoplastic model of Herschel-Bulkley (Herschel and Bulkley 1926).  $k$  represents the apparent viscosity and  $n$  the power-law term of the rheological behavior.

3) The structure parameter

Equation (10) represents the approach to the structure parameter, where  $t_{eq}$  is the characteristic time. The first term on the right-hand side is the structure buildup and the second term the breakdown. Equation (11) is the final equation presented by de Souza Mendes and Thompson (2013).

**Fig. 16** Analysis of the influence of the empirical parameter  $a$  for the shear rate of  $0.01 \text{ s}^{-1}$

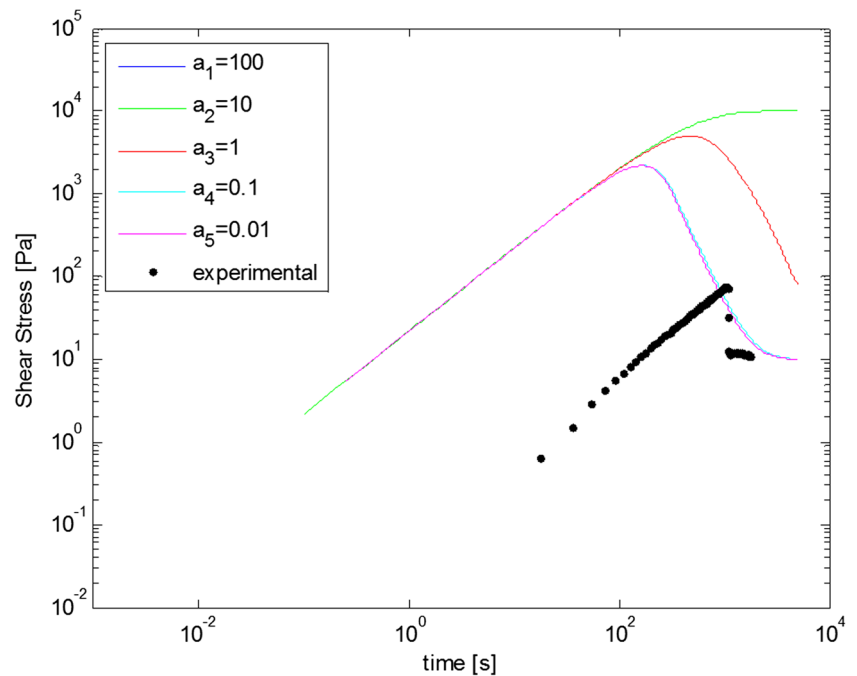
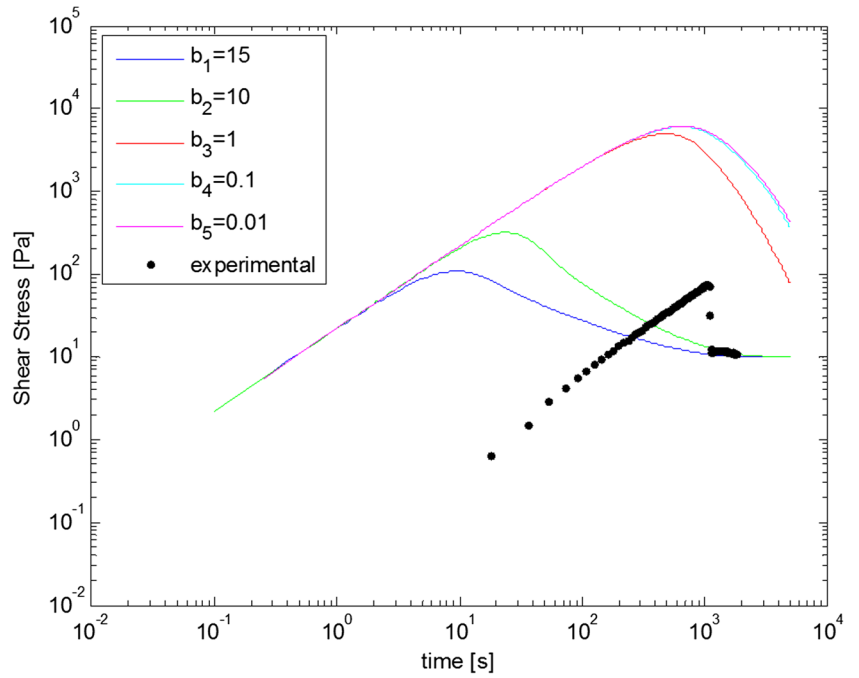


**Fig. 17** Analysis of the influence of the empirical parameter  $b$  for the shear rate of  $0.01 \text{ s}^{-1}$



$$\frac{d\lambda}{dt} = \frac{1}{t_{eq}} \left( \left( \frac{1}{\lambda} - \frac{1}{\lambda_0} \right)^a - f(\tau)\lambda^b \right) \tag{9}$$

**Numerical solution**

Euler’s numerical method was used to solve the differential equations. First, to validate the algorithm, the simulation was made with the parameter values described in de Souza Mendes and Thompson (2013). Figure 10 shows a dimensionless curve that represents the time evolution of stress for

$$\frac{d\lambda}{dt} = \frac{1}{t_{eq}} \left[ \left( \frac{1}{\lambda} - \frac{1}{\lambda_0} \right)^a - \left( \frac{\lambda}{\lambda_{eq}(\tau)} \right)^b \left( \frac{1}{\lambda_{eq}(\tau)} - \frac{1}{\lambda_0} \right)^a \right] \tag{10}$$

**Fig. 18** Analysis of the influence of the empirical parameter  $t_{eq}$  for the shear rate of  $0.01 \text{ s}^{-1}$

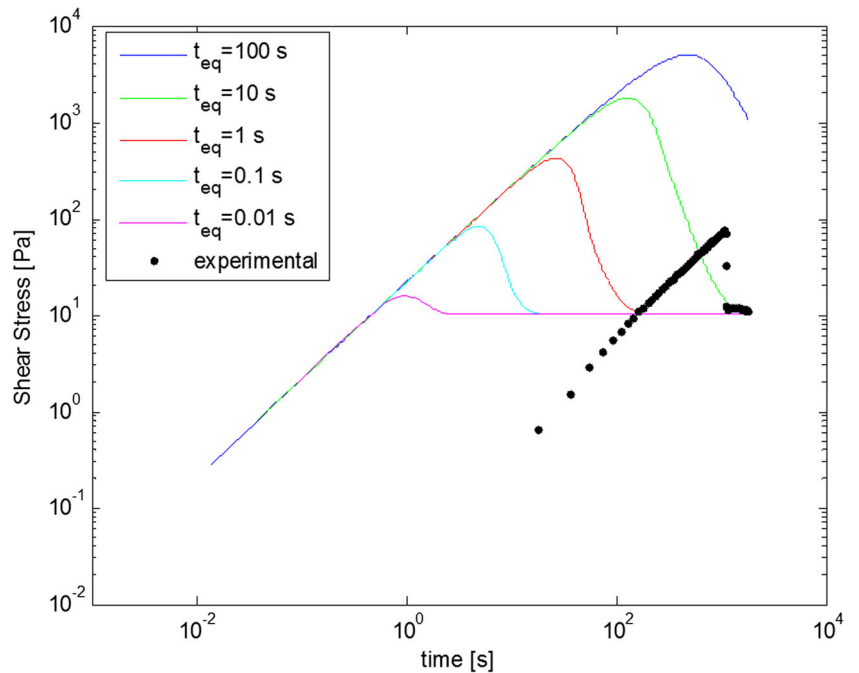
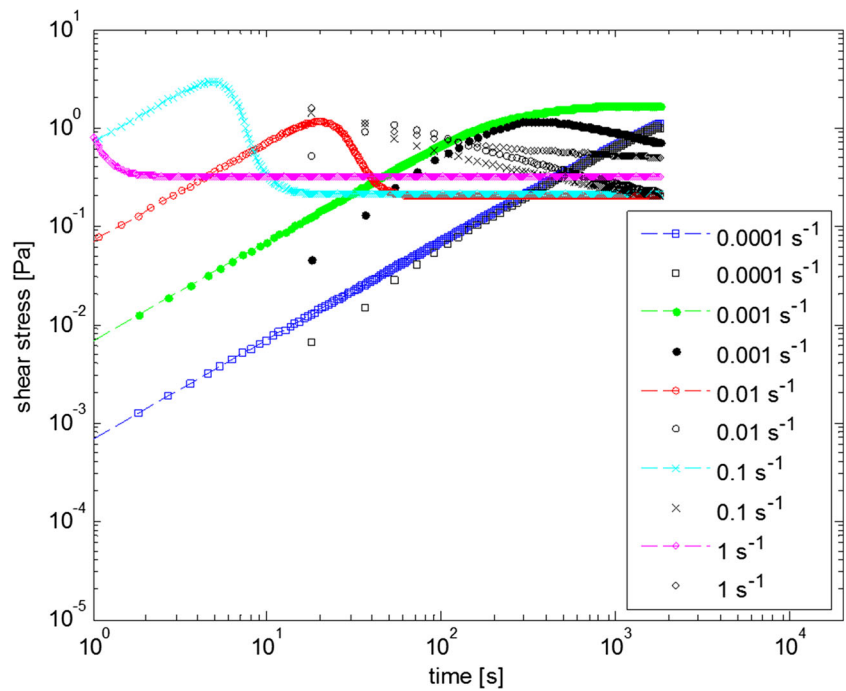


**Fig. 19** Stress evolution for oil 1 and 1 h of aging time, for breakdown experiments



constant shear rates. The dimensionless time has a specific shear rate defined by de Souza Mendes (2009) which represents the beginning of the power law region in a steady-state curve. The difference for small shear rate is almost none. Thus, the algorithm was considered to be coherent and subsequently applied during the analysis described in the sections that follow.

**Rheological parameters**

Figures 11 and 12 show the experimental results and Herschel-Bulkley fit. Finally, the curves show the simulation of a Newtonian fluid with very high viscosity, which is a feature of an apparent yield stress material. Tables 1 and 2 report the parameters obtained. All the parameters were obtained with the least square method.

At this point, it is worth pointing out that the steady-state curve is not a stable curve. It has been discussed in other studies (Chang et al. 1998; de Souza Mendes 2009) and been experimentally proven for these oils on Luthi (2013) that is why the rest of the parameters are not obtained using this approach. Oscillatory tests are more reliable (see Fig. 13),

**Table 6** Empirical parameters from the transient experiments for oil 1 and 1 h of aging time

Parameters	Values	Units
<i>m</i>	14.29	–
<i>a</i>	1.2	–
<i>b</i>	1.2	–
<i>t<sub>eq</sub></i>	0.41	s

and they were carried out to obtain the parameters of the model, as discussed by Chang et al. (1998), de Souza Mendes (2009), and Luthi (2013).

A and B are the transition points. Point B is the static limit, defined as  $\tau_y$ . Storage modulus is the plateau value for  $G'$  in Fig. 13, which is mathematically defined in Eq. (12). Final viscosity  $\eta_{\infty}$  can be obtained from Eq. (13) by the classic loss modulus.

$$\lim_{\lambda \rightarrow \lambda_0} G' = G_0 \tag{11}$$

$$\lim_{\lambda \rightarrow \lambda_0} G'' = \omega \eta_{\infty} \tag{12}$$

These tests were carried out for both oil samples for several aging times. The results for oil 1 and oil 2 for 1 h of aging are shown in Tables 3 and 4, respectively.

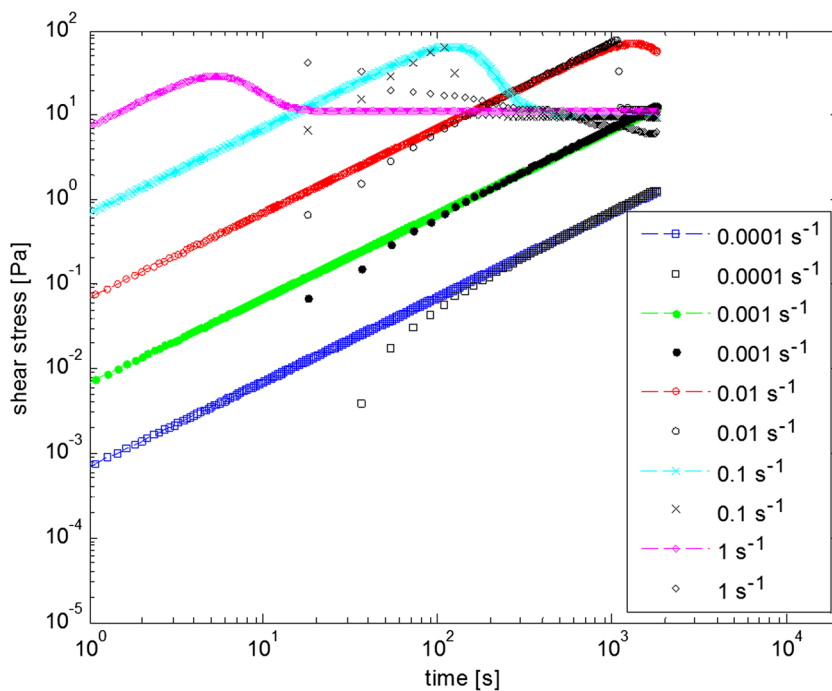
**Comparison model versus experiments**

After the parameters with physical meaning have been obtained, it is necessary to obtain the empirical ones. The least

**Table 7** Empirical parameters from the transient experiments for oil 2 and 1 h of aging time

Parameters	Values	Units
<i>m</i>	314.19	–
<i>a</i>	3	–
<i>b</i>	3	–
<i>t<sub>eq</sub></i>	0.41	s

**Fig. 20** Stress evolution for oil 2 and 1 h of aging time, for breakdown experiments



square method was applied to the transient experiments. The main problem is that the model cannot reproduce the experimental data with accuracy. As shown in Fig. 14, in the test of constant shear rate, the variation of the shear stress with time has—regardless of the range of the empirical parameters—a delay from the data to the model.

Figure 14 compares the experimental results with the simulation ones, for empirical parameters equal to the ones reported in the literature by de Souza Mendes and Thompson (2013). The values of the empirical parameters are shown in Table 5.

**Empirical parameters**

A sensitivity analysis was performed covering a large domain of each parameter to show that the empirical parameters could

**Table 8** Stress overshoot error comparing the simulation with the experimental data for oil 2

Stress overshoot				
Shear rate (s <sup>-1</sup> )	Experimental (Pa)	Model (Pa)	Error (Pa)	Error %
1	42.11	28.50	13.62	47
0.1	63.55	65.40	1.85	2.8
0.01	77.13	69.93	7.20	10.3
0.001	13.08	12.49	0 <sup>a</sup>	0 <sup>a</sup>
0.0001	1.29	1.25	0 <sup>a</sup>	0 <sup>a</sup>

<sup>a</sup> For shear rates of 0.001 and 0.0001 the stress overshoot was not reached, neither in the experiment nor in the model, that is why there is no error

not reproduce the experimental data. Figures 15, 16, 17, and 18 show the impact of each parameter on the results for a shear rate of 0.01 s<sup>-1</sup>. The other parameters were kept constant at the values displayed in Table 5.

None of the empirical parameters delays the whole curve to fit the experimental data. This occurs because none of them directly influences the elastic behavior.

**Modification of the model**

We propose to modify the model by adding another empirical parameter in the elastic term; in this way, the trend would be maintained, and the shear stress slope could change with time.

This generalization does not disrupt the physical meaning of the equation for the following reason: Although it is no longer the only parameter, the elastic behavior is still directly

**Table 9** The error of the time to reach the overshoot of the simulation with the experimental data for oil 2

Time to reach the overshoot				
Shear rate (s <sup>-1</sup> )	Experimental (s)	Model (s)	Error (s)	Error %
1	18	15.31	2.69	14.9
0.1	108	130.15	22.15	20.5
0.01	1062	1.334.3	272.35	25.6
0.001	1782	1782	0 <sup>a</sup>	0 <sup>a</sup>
0.0001	1782	1782	0 <sup>a</sup>	0 <sup>a</sup>

<sup>a</sup> For shear rates of 0.001 and 0.0001 the stress overshoot was not reached, neither in the experiment nor in the model, that is why there is no error

**Table 10** Empirical parameters from the transient experiments for oil 2 and 5 h of aging time

Parameters	Values	Units
$m$	619	–
$a$	3	–
$b$	3	–
$t_{eq}$	0.41	s

proportional to the storage modulus, but the relation between the variation of the structure parameter and the variation of the elastic response is not representable by the initial formulation. In other words, the spring constant has decreased, and the elastic response to stress is not as strong as proposed by de Souza Mendes and Thompson (2013).

The most generic solution would be to add one parameter, resulting in Eq. (14).

$$G_s = \left(\frac{G_0}{m_{new}}\right) e^{m_{old} \left(\frac{1}{\lambda} - \frac{1}{\lambda_0}\right)} \tag{13}$$

In our case, the influence of parameter  $m_{old}$  can be held by parameters  $a$  and  $b$ , as can be seen in Figs. 15, 16, and 17 and we simply reformulate Eq. (13), removing parameter  $m_{old}$ . The result can be seen in Eq. (14). This has been done because one of the main comparisons about all the models is how many empirical parameters they have. One of the best aspects about the model proposed by de Souza Mendes and Thompson (2013) is the reduced number.

$$G_s = \left(\frac{G_0}{m}\right) e^{\left(\frac{1}{\lambda} - \frac{1}{\lambda_0}\right)} \tag{14}$$

All the equations of the modified Souza Mendes and Thompson model are summarized here for better visualization.

$$\frac{\theta_2}{\eta_\infty} \left(\frac{\tau}{\theta_1} + \dot{\tau}\right) = (\dot{\gamma} + \theta_2 \cdot \ddot{\gamma}) \tag{1}$$

$$\theta_1 = \left(1 - \frac{\eta_\infty}{\eta_V(\lambda)}\right) \frac{\eta_V(\lambda)}{G_s(\lambda)} \tag{2}$$

$$\theta_2 = \left(1 - \frac{\eta_\infty}{\eta_V(\lambda)}\right) \frac{\eta_\infty}{G_s(\lambda)} \tag{3}$$

$$G_s = \left(\frac{G_0}{m}\right) e^{\left(\frac{1}{\lambda} - \frac{1}{\lambda_0}\right)} \tag{14}$$

$$\eta_V(\lambda) = \eta_\infty e^\lambda \tag{5}$$

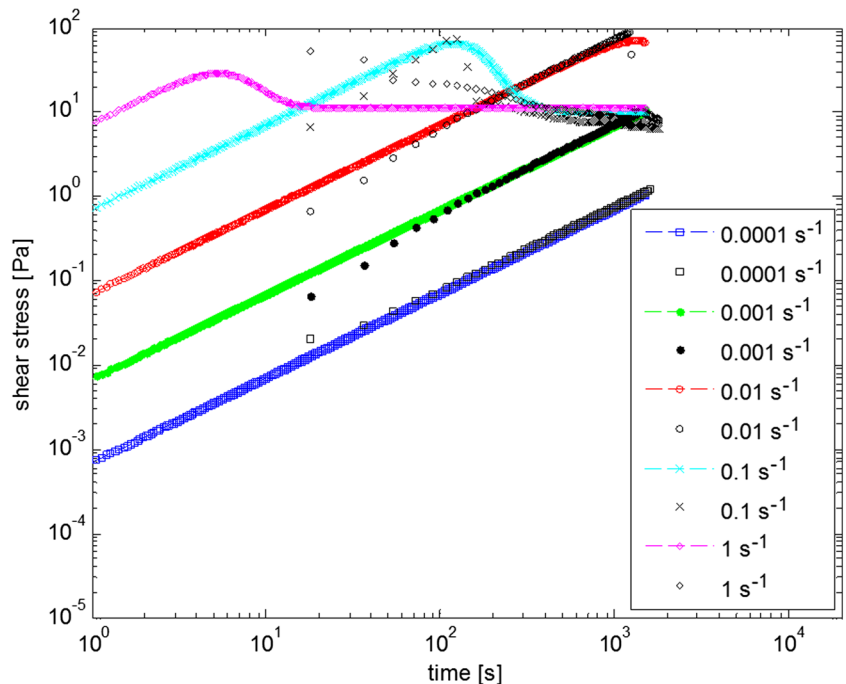
$$\lambda_{eq} = \ln\left(\frac{\eta_{eq}}{\eta_\infty}\right) \tag{6}$$

$$\lambda_0 = \ln\left(\frac{\eta_0}{\eta_\infty}\right) \tag{7}$$

$$\eta_{eq}(\dot{\gamma}) = \left(1 - e^{-\frac{\eta_0}{\dot{\gamma}}}\right) \left(\frac{\tau_y - \tau_{yd}}{\dot{\gamma}} e^{-\frac{\tau}{\tau_{yd}}} + \frac{\tau_{yd}}{\dot{\gamma}} + K \dot{\gamma}^{n-1}\right) + \eta_\infty \tag{9}$$

$$\frac{d\lambda}{dt} = \frac{1}{t_{eq}} \left[ \left(\frac{1}{\lambda} - \frac{1}{\lambda_0}\right)^a - \left(\frac{\lambda}{\lambda_{eq}(\tau)}\right)^b \left(\frac{1}{\lambda_{eq}(\tau)} - \frac{1}{\lambda_0}\right)^a \right] \tag{11}$$

**Fig. 21** Stress evolution for oil 2 and 5 h of aging time, for breakdown experiments



## Results and discussion

After the algorithm with the new equation is developed, the results are more coherent with the experimental data. Figure 19 shows that all the elastic behavior is better predicted by the modeling. The final shear stress is also predicted. The main point is the prediction of the overshoot.

The values of the empirical parameters were calculated by the least square method with the data of the experiment with shear rate of  $0.01 \text{ s}^{-1}$ ; once the parameters were calculated, we simulated the results with the other shear rates. The final results can be seen in Table 6 and Fig. 19 for oil 1 and Table 7 and Fig. 20 for oil 2.

After the elastic and the dynamic shear stress are calculated with good accuracy, the next goal is to see how accurate the model can predict the overshoot point. Table 8 shows the error for oil 2. Table 9 shows the error of the time necessary to reach the maximum stress, where the solid-like behavior turns liquid-like.

The error goes up as the shear rate rises. This happens because the empirical parameters were calculated with a shear rate of  $0.01 \text{ s}^{-1}$  and used in the simulation of all the other shear rates. To decrease the error, we should calculate the empirical parameters for each curve of constant shear rate.

The idea is a procedure for the industry; we want to verify if it is possible to do only one kinetic test and be able to predict the behavior of the gelled crude. The error rises as the difference between the actual shear rate and the one used to calculate the empirical parameter rises. For the industry, when trying to simulate the restart, the results we obtained are reasonable, since the shear rate's domain of the problem is up to  $0.1 \text{ s}^{-1}$ .

The model's idea is to simulate the oil's behavior independently of aging time. Hence, once the empirical parameters were calculated ( $a$ ,  $b$ ,  $t_{eq}$ ), they were not modified, even if that generated a high error. The only one that could not be kept constant was  $m$ . But the ratio  $\frac{G_0}{m}$  remained constant. In Table 10 and Fig. 21, we show the results for oil 2 for 5 h of aging time. The mean of the oscillatory test results is  $G_0=4333 \text{ Pa}$ .

We observed that independently of the oil and of the aging time, the result of the ratio of the storage modulus by the empirical parameter  $m$  is  $\frac{G_0}{m} \approx 7$ .

The same procedure was done for both oil samples for all the aging times, and the ratio was always the same. This is an unusual result, probably a coincidence, but it could also be evidence of constant for all waxy crudes. To ascertain that possibility, many more tests with different oil samples and other materials are needed.

## Final remarks

Rheological studies with two commercial waxy crude oil samples were performed to verify and define their rheological behavior under yielding at low temperature. This subject is very important to restart of blocked subsea flowlines with gelled waxy crudes.

There are available physical models to represent and explain the rheology during yielding. The model applied in this paper is a modification of de Souza Mendes and Thompson (2013). The alterations proposed do not affect the physical meaning of the parameters, but fit better our experimental results.

The comparison of the proposed model versus experimental data shows an acceptable error when predicting the elastic phase of the flow and the final viscous flow (up to 15 % error for both oil samples, independent of aging time). The highest error occurred when simulating the value of the shear stress and the time dependence (35 % for oil 1 with 5 h of aging time).

The ratio of the storage modulus to the parameter  $m$  obtained is the same for both oil samples at all aging times. A possible explanation is that there might be a constant related to the paraffins that relates the “spring constant” with the variation of the structure parameter. To generalize this conclusion, more tests are needed using different oil samples, and aging times.

For practical use, this model can be implemented in a generic simulator to address restart conditions, as long as sufficient experimental information is available to quantify the parameters that are not universal.

**Acknowledgments** The authors would like to thank PRH-ANP and Repsol-Sinopec-Brazil, for the financial support to this work.

## References

- Ajienka JA, Ikoku CU (1991) The effect of temperature on the rheology of waxy crude oils
- Barnes HA (1997) Thixotropy—a review. *J Non-Newtonian Fluid Mech* 70(1):1–33
- Barnes HA (1999) The yield stress—a review or ‘παντα ρει’—everything flows? *J Non-Newtonian Fluid Mech* 81(1):133–178
- Barnes HA, Walters K (1985) The yield stress myth? *Rheol Acta* 24(4):323–326
- Chang C, Boger DV, Nguyen QD (1998) The yielding of waxy crude oils. *Ind Eng Chem Res* 37(4):1551–1559
- Chang C, Nguyen QD, Rønningsen HP (1999) Isothermal start-up of pipeline transporting waxy crude oil. *J Non-Newtonian Fluid Mech* 87(2):127–154
- da Silva JAL, Coutinho JA (2004) Dynamic rheological analysis of the gelation behaviour of waxy crude oils. *Rheol Acta* 43(5):433–441
- Davidson MR, Dzuy Nguyen Q, Chang C, Rønningsen HP (2004) A model for restart of a pipeline with compressible gelled waxy crude oil. *J Non-Newtonian Fluid Mech* 123(2):269–280
- de Souza Mendes PR (2009) Modeling the thixotropic behavior of structured fluids. *J Non-Newtonian Fluid Mech* 164(1):66–75



- de Souza Mendes PR (2011) Thixotropic elasto-viscoplastic model for structured fluids. *Soft Matter* 7(6):2471–2483
- de Souza Mendes PR, Thompson RL (2012) A critical overview of elasto-viscoplastic thixotropic modeling. *J Non-Newtonian Fluid Mech* 187:8–15
- de Souza Mendes PR, Thompson RL (2013) A unified approach to model elasto-viscoplastic thixotropic yield-stress materials and apparent yield-stress fluids. *Rheol Acta* 52(7):673–694
- Dullaert K, Mewis J (2005) A model system for thixotropy studies. *Rheol Acta* 45(1):23–32
- Dullaert K, Mewis J (2006) A structural kinetics model for thixotropy. *J Non-Newtonian Fluid Mech* 139(1):21–30
- Herschel WH, Bulkley R (1926) Konsistenzmessungen von Gummi-Benzollösungen. *Kolloid Z* 39:291–300
- Lee HS (2008). Computational and rheological study of wax deposition and gelation in subsea pipelines. ProQuest
- Luthi IF (2013). Rheological characterization of a waxy crude oil and experimental study of the restart of a line blocked with gelled waxy crude. Campinas: Faculty of Mechanical Engineering, State University of Campinas, 124 p. Master Thesis
- Mewis J (1979) Thixotropy—a general review. *J Non-Newtonian Fluid Mech* 6(1):1–20
- Mewis J, Wagner NJ (2009) Thixotropy. *Adv Colloid Interf Sci* 147:214–227
- Mujumdar A, Beris AN, Metzner AB (2002) Transient phenomena in thixotropic systems. *J Non-Newtonian Fluid Mech* 102(2):157–178
- Phillips DA, Forsdyke IN, McCracken IR, Ravenscroft PD (2011a) Novel approaches to waxy crude restart: part 1: thermal shrinkage of waxy crude oil and the impact for pipeline restart. *J Pet Sci Eng* 77(3):237–253
- Phillips DA, Forsdyke IN, McCracken IR, Ravenscroft PD (2011b) Novel approaches to waxy crude restart: part 2: an investigation of flow events following shut down. *J Pet Sci Eng* 77(3):286–304
- Slibar A, Paslay PR (1963) Steady-state flow of a gelling material between rotating concentric cylinders. *J Appl Mech* 30(3):453–460
- Srivastava SP, Handoo J, Agrawal KM, Joshi GC (1993) Phase-transition studies in alkanes and petroleum-related waxes—a review. *J Phys Chem Solids* 54(6):639–670
- Thewlis J (1962) Oxford encyclopedia dictionary of physics
- Tiu C, Boger DV (1974) Complete rheological characterization of time-dependent food products. *J Texture Stud* 5(3):329–338
- Toorman EA (1997) Modelling the thixotropic behaviour of dense cohesive sediment suspensions. *Rheol Acta* 36(1):56–65
- Vinay G, Wachs A, Frigaard I (2009) Start-up of gelled waxy crude oil pipelines: a new analytical relation to predict the restart pressure. In: Asia Pacific Oil and Gas Conference & Exhibition. Society of Petroleum Engineers